Contribution from the School of Chemistry, Georgia Institute of Technology, Atlanta, Georgia 30332, and Istituto di Teoria e Struttura Elettronica e Comportamento Spettrochimico dei Composti di Coordinazione (CNR), Area della Ricerca di Roma, 00016 Monterotondo Stazione, Rome, Italy

Spectroelectrochemistry of (μ-Oxo)bis[(phthalocyaninato)iron(III)]

Lawrence A. Bottomley,*† Claudio Ercolani,*‡ Jean-Noel Gorce,† Giovanna Pennesi,‡ and Gentilina Rossi‡

Received August 19, 1985

The electrochemical behavior of (μ-oxo)bis[(phthalocyaninato)iron(III)], $[(Pc)Fe]_2O$, was studied in neat pyridine at a Pt-button electrode. Two single-electron-oxidation and two single-electron-reduction processes were observed for the dimer within the accessible potential range of the solvent. Variable-potential sweep rate cyclic voltammetric experiments verified the chemical reversibility of the oxidation process and the chemical irreversibility of the first reduction process at short times. Spectroelectrochemistry confirmed the long-term stability of the oxidation product and the short-lived nature of the reduction product, which decomposes ultimately to the iron phthalocyanine monomer. An electron-transfer pathway based upon the combined voltammetric, spectroelectrochemical, and coulometric results is proposed and compared to that observed for the analogous porphyrin complex (μ-oxo)bis[(tetraphenylporphinato)iron(III)], $[(TPP)Fe]_2O$.

Introduction

Three complexes are known in which two iron porphyrins are linked via the iron centers by a single atom: (μ-oxo), (μ-nitrido)-, and (μ-carbido)bis[(porphinato)iron], abbreviated $[(POR)Fe]_2O$, $[(POR)Fe]_2N$, and $[(POR)Fe]_2C$, respectively. Interestingly, the synthetic routes to these complexes are totally unrelated but can be accomplished in a straightforward manner. Treatment of ferric porphyrin with hydroxide[1] yields the μ-oxo dimer quantitatively. The μ-nitrido dimer is formed by the thermal decomposition of the ferric azide monomer.[2] The μ-carbido dimer is formed by reaction of CI_4 with the monomeric ferrous porphyrin under reducing conditions.[3] All three dimeric complexes are thermally stable and readily recovered in high purity from the reaction mixtures. The physicochemical properties of these complexes have been the subject of considerable interest.[2,4-13]

Recently, the preparation of single atom bridged dimers of iron phthalocyanine have been described.[14,15] Iron phthalocyanine, (Pc)Fe, is indefinitely stable in air as a pure solid. However, when in contact with a variety of solvents (e.g. dimethylformamide, dimethyl sulfoxide, dioxane, and tetrahydrofuran) (Pc)Fe reacts with O_2 to form a μ-oxo dimer,[14] $[(Pc)Fe]_2O$. Two different crystalline forms of this complex have been observed. The μ-nitrido homologue has been prepared by treating a suspension of (Pc)Fe in boiling α-chloronaphthalene with an excess of NaN_3.[15]

Unlike the corresponding porphyrin dimers, both $[(Pc)Fe]_2O$ and $[(Pc)Fe]_2N$ are highly insoluble in nondonor solvents and only slightly soluble in liquid nitrogenous bases. The μ-nitrido complex is indefinitely stable in these media. In contrast, prolonged contact with pyridine (py) liquid or vapor at room temperature under aerobic conditions transformed $[(Pc)Fe]_2O$ first to a dipyridinated complex and ultimately to $(Pc)Fe(py)_2$ with release of the bridging atom. Experiments with isotopically enriched ^{18}O as the bridging moiety have conclusively demonstrated that O_2 was not produced in this reaction. When the μ-oxo dimer was treated with py in the presence of triphenylphosphine (PPh_3), $OPPh_3$ was obtained.[16]

We have recently examined the redox reactivity of $[(Pc)Fe]_2N$ in pyridine.[15b] The dimeric integrity of this complex was maintained during the electrogeneration of both the dimer cation and the dimer anion. As the μ-oxo complex is isoelectronic with the μ-nitrido anion $\{[(Pc)Fe]_2N\}^-$, one might predict that oxidation of the μ-oxo complex should result in the formation of a stable cation, $\{[(Pc)Fe]_2O\}^+$. The aim of the present study was to examine the electroreactivity of $[(Pc)Fe]_2O$ in pyridine and to compare the reactivity with that observed for $[(Pc)Fe]_2N$ and the μ-oxo dimer of iron tetraphenylporphyrin, $[(TPP)Fe]_2O$.

Experimental Section

Preparation and purification of solid samples of $[(Pc)Fe]_2O$, as either μ-oxo type I (with characteristic infrared bands at 852 and 824 cm^{-1}) or μ-oxo type II, were performed as described previously.[14] μ-Oxo type I was mainly used in the electrochemical experiments presented here. Identical electrochemical behavior was found with samples of μ-oxo type II, as expected, since the two crystalline isomers have the same composition and give rise to the same species in pyridine solution.[14] Mekhryakova et al.,[17] referring to part of our work,[14a] have recently suggested an alternative formulation for $[(Pc)Fe]_2O$, i.e. $H_2\{[(Pc)Fe]_2O\}$ (containing Fe(II)), on the basis of their results regarding the corresponding species having *tert*-butyl substituents on the peripheral benzene rings of the phthalocyanine molecule. That formulation is clearly erro-

† Georgia Institute of Technology.
‡ Istituto di Teoria e Struttura Elettronica.

(1) Cohen, I. A. *J. Am. Chem. Soc.* **1969**, *91*, 1980.
(2) (a) Summerville, D. A.; Cohen, I. A. *J. Am. Chem. Soc.* **1976**, *98*, 1747-1752. (b) Scheidt, W. R.; Summerville, D. A.; Cohen, I. A. *J. Am. Chem. Soc.* **1976**, *98*, 6623-6628.
(3) Mansuy, D.; Lecomte, J.-P.; Chottard, J.-C.; Bartoli, J.-F. *Inorg. Chem.* **1981**, *20*, 3119.
(4) (a) Hoffman, A. B.; Collins, D. M.; Day, V. W.; Fleischer, E. B.; Srivastava, T. S.; Hoard, J. L. *J. Am. Chem. Soc.* **1972**, *94*, 3620. (b) Cohen, I. A. *Struct. Bonding (Berlin)* **1980**, *40*, 1. (c) Smith, P. D.; James, B. R.; Dolphin, D. H. *Coord. Chem. Rev.* **1981**, *39*, 31. (d) Adar, F.; Srivastava, T. S. *Proc. Natl. Acad. Sci. U.S.A.* **1975**, *72*, 4419. (e) Burke, J. M.; Kincaid, J. R.; Spiro, T. G. *J. Am. Chem. Soc.* **1978**, *100*, 6077.
(5) (a) Schick, G. A.; Bocian, D. F. *J. Am. Chem. Soc.* **1980**, *102*, 7982-7984. (b) *Ibid.* **1983**, *105*, 1830-1838. (c) Schick, G. A.; Findsen, E. W.; Bocian, D. F. *Inorg. Chem.* **1982**, *21*, 2885-2887.
(6) (a) Kadish, K. M.; Cheng, J. S.; Cohen, I. A.; Summerville, D. A. *ACS Symp. Ser.* **1977**, *No. 38*, Chapter 5. (b) Kadish, K. M.; Bottomley, L. A.; Brace, J. G.; Winograd, N. J. *J. Am. Chem. Soc.* **1980**, *102*, 4341-4344. (c) Kadish, K. M.; Rhodes, R. K.; Bottomley, L. A.; Goff, H. M. *Inorg. Chem.* **1981**, *20*, 3195-3200.
(7) Bottomley, L. A.; Garrett, B. B. *Inorg. Chem.* **1982**, *21*, 1260.
(8) (a) English, D. R.; Hendrickson, D. N.; Suslick, K. S. *Inorg. Chem.* **1983**, *22*, 367-368. (b) Bocian, D. F.; Findsen, E. W.; Hofmann, J. A., Jr.; Schick, G. A.; English, D. R.; Hendrickson, D. N.; Suslick, K. S. *Inorg. Chem.* **1984**, *23*, 800-807. (c) English, D. R.; Hendrickson, D. N.; Suslick, K. S. *Inorg. Chem.* **1985**, *24*, 121-122.
(9) Lancon, D.; Kadish, K. M. *Inorg. Chem.* **1984**, *23*, 3942-3947.
(10) (a) Phillippi, M. A.; Shimomura, E. T.; Goff, H. M. *Inorg. Chem.* **1981**, *20*, 1322. (b) Phillippi, M. A.; Goff, H. M. *J. Am. Chem. Soc.* **1982**, *104*, 6024. (c) Shimomura, E. T.; Phillippi, M. A.; Goff, H. M. *J. Am. Chem. Soc.* **1981**, *103*, 6778. (d) Phillippi, M. A.; Goff, H. M. *J. Am. Chem. Soc.* **1979**, *101*, 7641-7643.
(11) (a) Kadish, K. M.; Larsen, G.; Lexa, D.; Momenteau, M. *J. Am. Chem. Soc.* **1975**, *97*, 282. (b) Chang, D.; Cocolios, P.; Wu, Y. T.; Kadish, K. M. *Inorg. Chem.* **1984**, *23*, 1629-1633.
(12) Wenk, S. A.; Schultz, F. A. *J. Electroanal. Chem. Interfacial Electrochem.* **1979**, *101*, 89.
(13) Goedken, V. L.; Deakin, M. R.; Bottomley, L. A. *J. Chem. Soc., Chem. Commun.* **1982**, 607.
(14) (a) Ercolani, C.; Rossi, G.; Monacelli, F. *Inorg. Chim. Acta* **1980**, *44*, L215-L216. (b) Ercolani, C.; Gardini, M.; Monacelli, F.; Pennesi, G.; Rossi, G. *Inorg. Chem.* **1983**, *22*, 2584-2589.
(15) (a) Goedken, V. L.; Ercolani, C. *J. Chem. Soc., Chem. Commun.* **1984**, 378-279. (b) Bottomley, L. A.; Gorce, J.-N.; Goedken, V. L.; Ercolani, C. *Inorg. Chem.* **1985**, *24*, 3733-3737.
(16) Ercolani, C.; Gardini, M.; Pennesi, G.; Rossi, G. *J. Chem. Soc., Chem. Commun.* **1983**, 549-550.
(17) Mekhryakova, N. G.; Bundina, N. I.; Gulina, T. Y.; Kaliya, O. L.; Lukyanets, E. A. *Zh. Obshch. Khim.* **1984**, *54*, 1656.

0020-1669/86/1325-2338$01.50/0

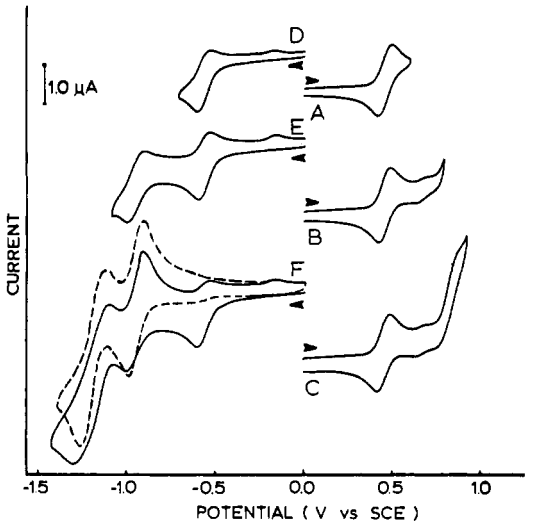

Figure 1. Cyclic voltammograms obtained on a 0.250 mM solution of $[(Pc)Fe]_2O$ in pyridine at a potential sweep rate of 200 mV s^{-1}. The initial potential was set at 0.00 V and the switching potential was 0.59 (A), 0.80 (B), 0.92 (C), −0.71 (D), −1.10 (E), and −1.42 V (F). The dashed voltammogram next to curve F was obtained after 10 continuous-potential sweeps between 0.00 and −1.42 V.

neous in the light of our previous work[14] and of the present electrochemical results. Recent contributions by other authors[18-20] give further support to the assumption of an Fe(III) μ-oxo dimeric structure. Recently, in a Mössbauer investigation,[21] lack of evidence for μ-oxo type II was reported following our methods of preparation for this crystalline isomer.[14] We confirm that μ-oxo type II can be easily obtained in a number of ways. We shall be referring to the above-mentioned contribution[21] in a forthcoming paper.

$[(TPP)Fe]_2O$ was prepared by the method of Adler and co-workers.[22] The supporting electrolytes, tetrabutylammonium perchlorate (TBAP) and tetraethylammonium perchlorate (TEAP), were obtained from the Eastman Chemical Co. Prior to use, TBAP and TEAP were recrystallized three times from absolute ethanol, dried in vacuo for 24 h at 100 °C, and stored in an evacuated desiccator. Pyridine was purchased from Mallinckrodt as reagent grade. This solvent was first treated with KOH and freshly distilled from CaO under N_2.

Voltammetric and spectroelectrochemical experiments were carried out with the equipment and techniques previously described.[15b,23] Since $[(Pc)Fe]_2O$ is unstable in py over time, voltammetric experiments were performed on freshly prepared solutions. Twenty minutes after dissolution of $[(Pc)Fe]_2O$, the solutions were discarded. All solutions were deoxygenated by passing a stream of solvent-saturated prepurified N_2 into the solution for at least 10 min prior to recording the voltammogram. To maintain an O_2-free environment, the solution was blanketed with N_2 during all experiments. Experiments were carried out at ambient temperature (23 ± 1 °C). All potentials reported herein were referenced to the SCE and were uncorrected for liquid-junction potentials. For interlaboratory comparison, the midpoint potential obtained for the ferrocenium ion/ferrocene couple was 0.45 V. The uncertainty in each potential reported herein is ±10 mV.

Results and Discussion

Electrochemistry of $[(Pc)Fe]_2O$. Figure 1 illustrates cyclic voltammograms typically obtained on a 0.25 mM solution of $[(Pc)Fe]_2O$ dissolved in 0.1 M TBAP/py. Two electrooxidation processes were observed when the potential was swept positively from 0.00 V. The first oxidation process was isolated by switching the potential sweep direction at 0.59 V. A variable-potential sweep rate study was performed over the potential sweep rate range of 0.02–9.9 V s^{-1}. Analysis of peak current and peak potential data as a function of sweep rate indicated the following trends: (a) $E_{1/2}$ was measured at +0.470 and was independent of sweep rate; (b) the cathodic to anodic peak current was equal to 1 at all sweep rates; (c) the anodic peak current was proportional to the square root of the potential sweep rate; (d) the potential separation between the anodic peak and the cathodic peak ranged from 62 (at V = 20 mV s^{-1}) to 131 mV (at V = 9.9 V s^{-1}), increasing with increasing sweep rate; (e) the peak shape ($E_{p,a} - E_{p/2}$) was consistently 63 ± 2 mV. These trends indicated that the first oxidation process was best described as the quasi-reversible abstraction of one electron from the dimer.

A second electrooxidation process was observed on the edge of the solvent potential window. Due to the overlap with the solvent discharge, a complete variable-potential sweep rate analysis was not possible. However, programmed differential-pulse voltammetric analysis of this process as per the method of Birke[24] indicated that $E_{1/2}$ = 0.87 V for this process.

Three electroreduction processes were observed when the potential was swept negatively from 0.00 V as depicted in Figure 1D–F. Analysis of the variable-potential sweep rate data on the first reduction process indicated the following trends: (a) The anodic to cathodic peak current ratio was 0.75 at a potential sweep rate of 20 mV s^{-1} and increased with increasing sweep rate. A ratio of 1 was obtained at sweep rates greater that 500 mV s^{-1}. (b) The ratio of the cathodic peak current to the square root of the potential sweep rate was not constant but decreased as the sweep rate increased. (c) $E_{p,c}$ shifted cathodically by 15 mV per decade of potential sweep rate. (d) At sweep rates greater than 500 mV s^{-1} the midpoint potential was measured at −0.59 V and was found to be independent of sweep rate. (e) At a sweep rate of 20 mV s^{-1}, the peak potential separation was 62 mV and the difference between $E_{p,c}$ and $E_{1/2}$ was 31 mV. These trends indicated that the first electroreduction of the dimer was best described as a reversible electron transfer followed by a chemical reaction.

The second reduction process was also examined by variable-potential sweep rate cyclic voltammetry. The ratio of the cathodic peak current for the second reduction over that measured for the first reduction decreased with increasing sweep rate. A value of 1 was obtained at sweep rates greater than 500 mV s^{-1}. This indicated that the chemical reaction that followed the first electron transfer could be eliminated at sweep rates greater than 500 mV s^{-1}. The midpoint potential was found to be independent of sweep rate and was measured at −0.95 V. When the potential sweep direction was reversed at −1.40 V, three cathodic and four anodic processes were observed (see Figure 1F). The current measured for the cathodic process at $E_{p,c}$ = −1.30 V was ~2.5 times that measured for the cathodic process at $E_{p,c}$ = −0.98 V. This indicated the passage of at least 2 equiv of charge. The increase in current at $E_{p,a}$ = −0.93 V and the decrease in current at $E_{p,a}$ = −0.56 V indicated that the dimeric structure does not survive the insertion of more than two electrons into the complex. Indeed, voltammograms taken at the steady state (see the dashed voltammogram in Figure 1F) gave only two reversible electron transfers at $E_{1/2}$ = −0.96 and −1.20 V, respectively. The currents for these two processes were equal and were measured at twice the magnitude of that measured for the first reduction of the dimer. The steady-state voltammogram was that characteristic of the monomer, $(Pc)Fe(py)_2$.[25]

It should be noted that a small anodic current measured at $E_{p,a}$ = −0.18 V was obtained whenever the potential sweep included at least one reduction process. The magnitude of the anodic current was always less than 0.3 times the cathodic current at $E_{p,c}$ = −0.62 V. Attempts to capture the corresponding cathodic couple to this oxidation process were successful on continuous scan at sweep rates greater than 2.0 V s^{-1}. The midpoint potential was

(18) Kalz, W.; Homborg, H. *Z. Naturforsch., B: Anorg. Chem., Org. Chem.* **1983**, *38B*, 470.
(19) Metz, J.; Schneider, O.; Hanack, M. *Inorg. Chem.* **1984**, *23*, 1065.
(20) Kennedy, B. J.; Murray, K. S.; Zwack, P. R.; Homborg, H.; Kalz, W. *Inorg. Chem.* **1985**, *24*, 3302–3305.
(21) Frampton, C. S.; Silver, J. *Inorg. Chim. Acta* **1984**, *81*, L29.
(22) (a) Adler, A. D.; Longo, F. R.; Finarelli, J. D.; Goldmacher, J.; Assour, J.; Korsakoff, L. *J. Org. Chem.* **1967**, *32*, 476. (b) Adler, A. D.; Longo, F. R.; Kampas, F.; Kim, J. J. *Inorg. Nucl. Chem.* **1970**, *32*, 2443–2448.
(23) Bottomley, L. A.; Deakin, M. R.; Gorce, J.-N. *Inorg. Chem.* **1984**, *23*, 3563–3571.
(24) Birke, R. L.; Kim, M.-H.; Strassfeld, M. *Anal. Chem.* **1981**, *53*, 852–857.
(25) Lever, A. B. P.; Wilshire, J. P. *Inorg. Chem.* **1978**, *17*, 1145–1149.

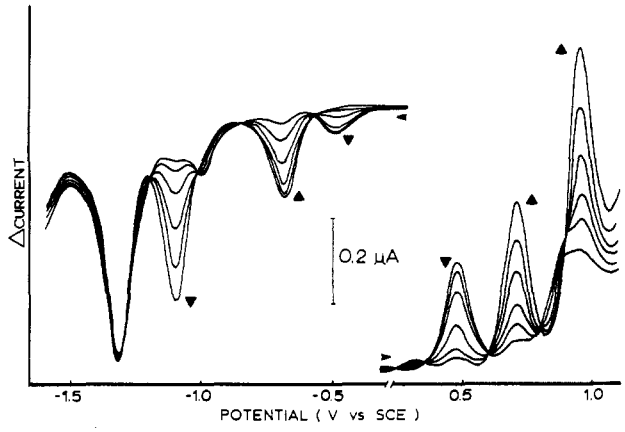

Figure 2. Differential-pulse voltammograms obtained on a 96.3 μM solution of $[(Pc)Fe]_2O$ in pyridine as a function of time after dissolution of the dimer. For each acquisition, the potential sweep rate was 50 mV s^{-1} and the pulse amplitude was 25 mV s^{-1}. The voltammograms displayed were recorded at 6-min intervals after dissolution of the dimer. After ca. 70 min decomposition of the dimer was complete. Between scans, the solution was purged with solvent-saturated N_2 for 15 s followed by a "rest" period of 15 s. The temperature of the solution was 22.0 ± 0.2 °C during the course of the experiment.

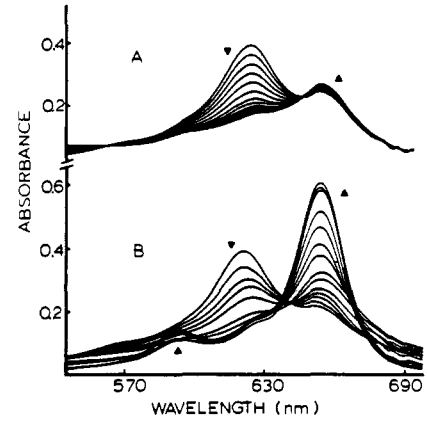

Figure 3. Visible spectra obtained during the electrolysis of a 0.27 mM solution of $[(Pc)Fe]_2O$ in pyridine at the OTTLE. Part A depicts the spectra obtained after the applied potential was stepped from E_{0c} to 0.59 V, generating the dimeric cation. Part B depicts the spectra obtained after the applied potential was stepped from E_{0c} to −0.70 V, generating, initially, the dimeric anion and ultimately the neutrally charged monomer $(Pc)Fe(py)_2$.

measured at −0.21 V. Addition of 1 equiv of water to the solution eliminated the cathodic peak regardless of sweep rate. The peak current, peak potential, and peak shape were also unaffected by the addition of PPh_3 to solution. The addition of OH^- (in the form of TBA^+OH^-) however, eliminated the process at $E_{1/2}$ = −0.21 V and produced a marked increase in the reversibility of the dimer reduction process at $E_{1/2}$ = −0.59 V.

During the course of the above experiments, the voltammetric behavior of the dimer changed with time. Figure 2 depicts a series of differential-pulse voltammograms obtained as a function of time on a fresh solution of the dimer. The initial two processes associated with the oxidation of the dimer (E_p = 0.47 and 0.87 V, respectively) decreased with the concomitant growth of two new processes characteristic of (Pc)Fe at E_p = 0.74 and 0.94 V. The two processes associated with reduction of the dimer (E_p = −0.68 and −1.00 V) decreased with the concomitant growth of the peak for reduction of the monomer (E_p = −1.11 V). Note that the data presented in Figure 2 was obtained with TEAP as the supporting electrolyte instead of TBAP. This change in the supporting electrolyte had no affect on the oxidation processes but did produce an anodic shift in the potentials for the reduction processes. For reference, reduction of (Pc)Fe in py that contains 0.1 M TEAP occurred at $E_{1/2}$ = −1.05 and −1.27 V. The rate of dimeric decomposition is dependent upon the method of solvent purification used. Analysis of the kinetics involved in the dimeric decomposition sequence is presently under study and will be published elsewhere.[26]

Spectroelectrochemistry of $[(Pc)Fe]_2O$. A 0.27 mM solution of $[(Pc)Fe]_2O$ in pyridine was placed in an optically transparent thin-layer electrochemical cell (OTTLE). At the potential of zero current, E_{0c}, (0.132 V) a spectrum characteristic of $[(Pc)Fe]_2O$ was obtained with an intense band at 622 nm and two shoulders at 569 and 653 nm. Stepping the applied potential to +0.55 V produced the immediate spectral changes depicted in Figure 3A. The 622-nm band lost intensity while a new band grew at 652 nm. Shoulders were formed at 624 and 692 nm. The interconversion was accomplished with isosbestic points at 563, 643, and 688 nm. No differences in the visible spectrum were observed over the wavelength range of 385–525 nm. The final stable spectrum was obtained within 40 s of electrolysis. This spectrum was unchanged for at least 10 min. After this time period gradual spectral decay was observed. Reversal of the potential within 10 min regenerated 98% of the starting material in the OTTLE. If the potential was reversed after 10 min, regeneration of the initial spectrum was accompanied by a diminished 622-nm band and a more intense 652-nm band.

The spectral changes observed on a fresh solution of $[(Pc)Fe]_2O$ after the application of a potential of −0.70 V are depicted in Figure 3B. For at least the first 12 s after the onset of the applied potential, the band at 622 nm lost intensity with a corresponding growth of a new band at 652 nm. This transformation was accompanied by isosbestic points at 548, 641, and 679 nm. After 12 s, the transformation was devoid of isosbestic points. The 622-nm band all but disappeared while the 652-nm band greatly intensified. A new low-intensity band appeared at 592 nm. The final spectrum compared favorably with that of $(Pc)Fe(py)_2$. Reversing the applied potential to 0.00 V did not produce any spectral changes. Stepping the applied potential to −1.10 V resulted in a rapid change in the color of the solution in the OTTLE from blue-green to pink and gave a spectrum characteristic of the Fe^I anion,[25] $\{(Pc)Fe\}^-$.

Electrochemistry of $[(TPP)Fe]_2O$. A number of workers have investigated the electroreductive behavior of $[(TPP)Fe]_2O$ in a variety of nonaqueous solvents.[10-12,27-29] Jones et al.[27] have depicted the voltammetry of $[(TPP)Fe]_2O$ in pyridine but did not provide an analysis of the mechanism. To permit the comparison of the electrode reactions between the Pc and TPP μ-oxo dimers, the electrochemistry of $[(TPP)Fe]_2O$ was investigated under the same conditions as employed above for $[(Pc)Fe]_2O$.

A 0.492 mM solution of $[(TPP)Fe]_2O$ in pyridine was examined voltammetrically. No well-defined oxidation processes were observed between 0.40 V and the anodic potential limit of the solvent. When the potential was swept negatively from 0.40 V, up to three reduction processes were observed. Figure 4 depicts the voltammograms obtained as a function of switching potential. The voltammograms depicted are similar to the voltammogram depicted by Jones et al.[27] Analysis of the first charge-transfer reaction in the manner presented above indicated that this process is best described as a reversible one-electron transfer with an $E_{1/2}$ = −1.03 V. When the switching potential is decreased to −1.55 V, a multielectron reduction wave is observed at $E_{p,c}$ = −1.44 V. As a consequence of this electroreduction, the anodic current coupled to the first reduction process is severely diminished and a new electron-transfer process occurs at $E_{p,a}$ = 0.15 V. This potential corresponds to that observed for the oxidation of $(TPP)Fe^{II}(py)_2$. When the switching potential is set at −1.80 V, a third electroreduction process is observed at $E_{p,c}$ = −1.66 V. This

(26) Ercolani, C.; Pennesi, G.; Rossi, G.; Monacelli, F., manuscript in preparation.

(27) Jones, S. E.; Srivastava, G. S.; Sawyer, D. T.; Traylor, T. G.; Mincey, T. C. *Inorg. Chem.* **1983**, *22*, 3903–3910.

(28) Felton, R. H.; Owen, G. S.; Dolphin, D.; Forman, A.; Borg, D. C.; Fajer, J. *Ann. N.Y. Acad. Sci.* **1973**, *206*, 504–510.

(29) Wolberg, A. *Isr. J. Chem.* **1974**, *12*, 1031.

third process corresponds to that observed for the Fe^I to Fe^I anion radical reduction for monomeric porphyrin in this solvent system.

A 0.12 mM solution of $[(TPP)Fe]_2O$ was placed in the OTTLE. When the applied potential was stepped from E_{0c} to −1.20 V, a rapid spectral transformation from the spectrum of the μ-oxo dimer to that characteristic of $(TPP)Fe^{II}(py)_2$ was observed. The species present in the OTTLE could not be oxidized until the applied potential was anodic of 0.30 V. Integration of the current during the reduction step confirmed the passage of 2 equiv of charge per dimer.

Electron-Transfer Pathways. On the basis of the results presented, the electron-transfer reactions of $[(Pc)Fe]_2O$ and $[(TPP)Fe]_2O$ can be accounted for by Schemes I and II, respectively. The midpoint potentials for each electron-transfer reaction are given on the reaction arrows, and the superscripted Roman numerals denote the formal valences assigned to each of the Fe atoms. It should be kept in mind that coordination of pyridine molecules at the external axial sites of the Fe atoms of the dimeric species occurs even though it has not been depicted in the schemes. The bis(pyridine) adduct of the μ-oxo dimer, $[(Pc)Fe(py)_2]_2O$, can be easily isolated in the solid state.[14]

Scheme I. Electrode Mechanism for $[(Pc)Fe]_2O$

$$\{[(Pc)Fe^{III,IV}]_2O\}^+ + e^- \xrightleftharpoons{0.47\ V} [(Pc)Fe^{III,III}]_2O$$

$$[(Pc)Fe^{III,III}]_2O + e^- \xrightleftharpoons{-0.59\ V} \{[(Pc)Fe^{II,III}]_2O\}^-$$

$$\{[(Pc)Fe^{II,III}]_2O\}^- + e^- \xrightleftharpoons{-0.95\ V} \{[(Pc)Fe^{II,II}]_2O\}^{2-}$$

at slow potential sweep rates or long times, the pathway for dimer decomposition is potential-dependent:

at $-0.59 \geq E \geq -0.95$ V

$$\{[(Pc)Fe^{II,III}]_2O\}^- + e^- \rightarrow 2(Pc)Fe^{II} + O^{2-}$$

at $-0.95 > E \geq -1.21$ V

$$\{[(Pc)Fe^{II,II}]_2O\}^{2-} + 2e^- \rightarrow 2\{(Pc)Fe^{I}\}^- + O^{2-}$$

at $E < -1.21$ V

$$\{[(Pc)Fe^{II,II}]_2O\}^{2-} + 4e^- \rightarrow 2\{(Pc)Fe^{I}\}^{2-} + O^{2-}$$

the electrogenerated monomeric material then undergoes the following reactions:

$$\{(Pc)Fe^{I}\}^- + e^- \xrightleftharpoons{-1.21\ V} \{(Pc)Fe^{I}\}^{2-}$$

$$(Pc)Fe^{II} + e^- \xrightleftharpoons{-0.96\ V} \{(Pc)Fe^{I}\}^-$$

$$(Pc)Fe^{III}(OH) + e^- \xrightleftharpoons{-0.21\ V} \{(Pc)Fe^{II}(OH)\}^-$$

Scheme II. Electron Mechanism for $[(TPP)Fe]_2O$

$$[(TPP)Fe^{III,III}]_2O + e^- \xrightleftharpoons{-1.03\ V} \{[(TPP)Fe^{II,III}]_2O\}^-$$

$$\{[(TPP)Fe^{II,III}]_2O\}^- + 3e^- \xrightarrow{E \leq -1.37\ V} 2\{(TPP)Fe^{I}\}^- + O^{2-}$$

the electrogenerated monomeric material then undergoes the following reactions:

$$(TPP)Fe^{II} + e^- \xrightleftharpoons{-1.32\ V} \{(TPP)Fe^{I}\}^-$$

$$\{(TPP)Fe^{III}\}^+ + e^- \xrightleftharpoons{0.18\ V} (TPP)Fe^{II}$$

For both schemes, the fate of the bridging atom is unknown at this time. Presumably, O^{2-} is not a stable entity in this medium and rapidly reacts with adventitious water to form OH_n^{n-2}.

Electrooxidation of $[(Pc)Fe]_2O$ is tentatively assigned as a metal-centered oxidation rather than a phthalocyanine ring-centered oxidation on the basis of the lack of any observable differences in the visible spectrum of the cation and the neutral complex over the region 400–550 nm. Lever has shown that this spectral region is diagnostic of ring- vs. metal-centered electron-transfer reactions.[30] We also explored this spectral region for the μ-nitrido complex and found no changes that identified a radical species being formed.[15b] The corresponding electron-transfer reaction for the porphyrin dimer has been assigned as ring-centered.[10b] Since the potential for this reaction is within 200 mV of that observed for the production of various metallophthalocyanine cation radicals[25,30] and phthalocyanines generally stabilize lower oxidation states of iron better than porphyrins, the assignment of an Fe(IV) center must be treated with reservation until a complete characterization of the cation is completed.

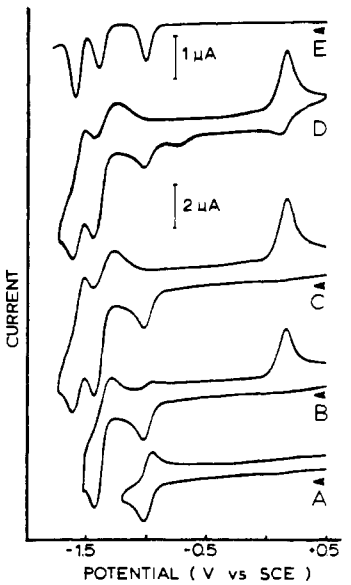

Figure 4. Cyclic and differential-pulse voltammetric data obtained on a 0.492 mM solution of $[(TPP)Fe]_2O$ in pyridine. Traces A–D are cyclic voltammograms obtained at a potential sweep rate of 200 mV s^{-1}. The potential sweeps were initiated at 0.50 V and the potential sweep direction was switched at −1.20 (A), −1.53 (B), and −1.74 V (C and D). Trace D is a cyclic voltammogram obtained at the steady state. Trace E is a differential-pulse voltammogram obtained at a potential sweep rate of 10 mV s^{-1}, a pulse amplitude of 25 mV, and a pulse frequency of 0.1 s.

Table I. Midpoint Potentials for the Dimers of Phthalocyanine and Tetraphenylporphyrin in Pyridine

	redox reaction[a]				
dimer	+2/+1	+1/0	0/−1	−1/−2	−2/−3
$[(Pc)Fe]_2O$	0.87	0.47	−0.59	−0.95	
$[(Pc)Fe]_2N$[b]		0.00	−0.83	−1.02	−1.29
$[(TPP)Fe]_2O$			−1.03	*e*	
$[(TPP)Fe]_2N$[b]		−0.25	−1.04	−1.52	−1.69
$[(TPP)Fe]_2C$[f]	1.03	0.52	−1.52[g]		
$[(Pc)Mn]_2O$[c]		0.35	−0.85[d]		

[a] Denotes charge on the dimer for the electrode reactant and electrode product. [b] Taken from ref 15b. [c] Taken from ref 32. [d] Multielectron process; see ref 32 for details. [e] Multielectron process; see text for details. [f] Taken from ref 9. [g] Multielectron process; see ref 9 for details.

Electroreduction of both $[(Pc)Fe]_2O$ and $[(TPP)Fe]_2O$ yields a dimer anion formally assigned as a mixed-valence Fe^{II}–Fe^{III} dimer. This assignment is in accord with the findings of Jones[27] and Kadish[11] for the porphyrin dimer in other nonaqueous solvents. Subsequent reduction of the porphyrin dimer initiates a decomposition pathway to the porphyrin monomeric species $\{(TPP)Fe^{I}\}^-$. The spectroelectrochemical data suggested that the mixed-valence anion is stable on the voltammetric time scale only. At longer times, the dimer dissociated into monomeric material. In contrast, subsequent reduction of the Pc dimer yielded a moderately stable (on the voltammetric time scale) dimeric dianion. This species has been assigned as an Fe^{II}–Fe^{II} dimer. Further reduction of

(30) Lever, A. B. P.; Licoccia, S.; Magnell, K.; Minor, P. C.; Ramaswamy, B. S. *Adv. Chem. Ser.* **1982**, *No. 201*, Chapter 11 and references therein.

the Pc dimer initiates dimeric decomposition to the monomeric Pc anion radical species $\{(Pc)Fe^{I}\}^{2-}$.

To facilitate comparisons, the midpoint potentials for the electrode reactions of the known single atom bridged dimers of Pc and TPP are listed in Table I. Interestingly, the electrode reactions of both $[(Pc)Fe]_2O$ and $[(Pc)Fe]_2N$ are anodic of the corresponding reactions of $[(TPP)Fe]_2O$ and $[(TPP)Fe]_2N$, respectively. This follows the trend previously observed for the monomeric complexes that the phthalocyanine ring stabilizes lower oxidation states of iron in phthalocyanine complexes as compared to the corresponding porphyrin complex.[30] Similarly, the midpoint potentials for $[(Pc)Fe]_2O$ are anodic of the corresponding couple for $[(Pc)Fe]_2N$. However, the potential differences decrease as the negative charge on the dimer increases. If one uses the MO diagram put forth for the TPP single atom bridged dimers[31] as a qualitative description of the MO diagram for the Pc single atom bridged dimers, then this trend is in accord with expectations. Also, one would predict that the HOMO for the μ-oxo complex is localized on the two metal atoms and the bridging moiety rather than the ring. Oxidation of the complex would then decrease the electron density about the metal atom. Note, however, that Hoffmann's MO diagram does not account for axial ligation of the Fe atoms by solvent molecules as has been shown to occur for $[(Pc)Fe]_2O$ by Ercolani et al.[14]

Comparison of the potentials for reduction of the isoelectronic dimers, $\{[(Pc)Fe]_2O\}^{+}$ to $[(Pc)Fe]_2N$, indicates that the μ-nitrido dimer is stabilized by 1300 mV over that of the analogous mixed-valence Fe^{III}–Fe^{IV} μ-oxo complex. This stabilization is significantly less than the value of 2050 mV observed by Kadish et al.[6] for the corresponding TPP dimers in the noncoordinating solvent CH_2Cl_2. This decrease may be a manifestation of the difference in the donor properties of the macrocycles or it may reflect the influence of a coordinating solvent.

Minor and Lever[32] have previously reported the electron-transfer mechanism of $[(Pc)Mn]_2O$ in pyridine. They observed one reversible oxidation at 0.35 V and a multielectron reduction to a monomeric anion radical species, $\{(Pc)Mn^{II}\}^{-}$, at -0.85 V. Their data is consistent only with an initial electron transfer involving two electrons, producing $\{[(Pc)Mn^{II}]_2O\}^{2-}$. No evidence for a mixed valence Mn^{III}–Mn^{II} species was obtained. This suggests that the potential for addition of the second electron to this complex must be equal to or anodic of the potential for addition of the first electron. For the corresponding Fe dimer described herein, two sequential one-electron reductions are observed, separated by 360 mV. Clearly, addition of electrons to either dimer populates an antibonding orbital, destabilizing the dimeric linkage. A rational explanation for the observed stabilization of the mixed-valence species for the Fe-containing dimer as compared to the Mn-containing dimer awaits the formulation of a MO description that accounts for changes in the identity of the central metal atom in the dimer, the presence of macrocycles with different donor properties, and the presence of nitrogenous bases producing perturbations at the axial positions of the dimer.

Acknowledgment. L.A.B. wishes to acknowledge the Istituto di Teoria e Struttura Elettronica, CNR, Area della Ricerca di Roma (Montelibretti), for a visiting professorship, kind hospitality, and excellent research facilities.

Registry No. $[(Pc)Fe]_2O$, 74353-48-3; $[(Pc)Fe]_2O^{+}$, 100228-78-2; $[(Pc)Fe]_2O^{-}$, 100228-80-6; $[(Pc)Fe]_2O^{2-}$, 100228-81-7; (Pc)Fe, 132-16-1; $(Pc)Fe^{-}$, 38600-22-5; $(Pc)Fe^{2-}$, 38600-23-6; (Pc)Fe(OH), 80602-48-8; $(Pc)Fe(OH)^{-}$, 100228-82-8; $[(TPP)Fe]_2O$, 12582-61-5; $[(TPP)Fe]_2O^{-}$, 54578-55-1; $(TPP)Fe^{-}$, 54547-68-1; (TPP)Fe, 16591-56-3; $(TPP)Fe^{+}$, 29484-63-7; $[(Pc)Fe]_2O^{2+}$, 100228-79-3; Bu_4NOH, 2052-49-5; $(Pc)Fe(py)_2$, 20219-84-5; pyridine, 110-86-1.

(31) Tatsumi, K.; Hoffmann, R. J. *J. Am. Chem. Soc.* **1981**, *103*, 3328-3341.

(32) Minor, P. C.; Lever, A. B. P. *Inorg. Chem.* **1983**, *22*, 826-830.

Contribution from the Chemistry Department,
The Ohio State University, Columbus, Ohio 43210

Multiple-Equilibria Model Describing the Axial Ligand Dependence of the Dioxygen Affinity of an Iron(II) Lacunar Complex. An Approach to the Regulation of Dioxygen Affinity

Kenneth A. Goldsby, Brian D. Beato, and Daryle H. Busch*

Received November 13, 1985

The dioxygen-binding behavior of the iron(II) lacunar complex chloro(3,11-dibenzyl-14,20-dimethyl-2,12-diphenyl-3,11,15,19,22,26-hexaazatricyclo[11.7.7.1^{5,9}]octacosa-1,5,7,9(28),12,14,19,21,26-nonaene-κ^4N)iron(II) hexafluorophosphate in 1.5 M 1-methylimidazole/acetonitrile (1.5 M MIM/AN) is described. Although 1-methylimidazole is known *not* to displace chloride as the axial ligand in acetonitrile (even at concentrations as high as 1.5 M), the lacunar iron(II) complex shows a high affinity for dioxygen in 1.5 M MIM/AN, in spite of the known low dioxygen affinity of the chloro complexes. The high dioxygen affinity of this system has been explained in terms of a trans displacement of the axial chloride by dioxygen. The displacement of chloride can occur via two pathways that incorporate two distinct types of equilibria: (1) equilibria involving the coordination of dioxygen and (2) equilibria involving the exchange of axial ligand. The entire process can be described by a multiple-equilibria model comprised of four separate, but mutually related, equilibria. To a first approximation, the functional dependence of dioxygen adduct formation on the concentration of dioxygen is the same as that expected for a single dioxygen equilibrium. For this reason, one may calculate a single effective binding constant that reflects the dioxygen affinity of this mixed-axial-ligand system. As expected from this model, the dioxygen affinity can be suppressed by the addition of excess chloride. The possibility of continuously regulating the dioxygen affinity over wide ranges by manipulating the concentrations of potential axial bases has been demonstrated, and applications are suggested.

Introduction

The dioxygen affinity of synthetic dioxygen carriers is known to be quite dependent upon the nature of the axial base. Basolo recognized that the equilibrium constant for dioxygen adduct formation (K_{O_2}) for a given cobalt Schiff-base complex varied with the axial base according to the $Co^{III/II}$ half-wave potential ($E_{1/2}$).[1] To account for the linear relationship between log K_{O_2} and $E_{1/2}$ for limited ranges of axial bases, the $Co^{III/II}$ half-wave potential

(1) (a) Carter, M. J..; Rillema, D. P.; Basolo, F. *J. Am. Chem. Soc.* **1974**, *96*, 392-400. (b) Carter, M. J.; Engelhardt, L. M.; Rillema, D. P.; Basolo, F. *J. Chem. Soc., Chem. Commun.* **1973**, 810-812.

0020-1669/86/1325-2342$01.50/0